AUGMENTED STATE-SPACE FORMULATION FOR THE STUDY OF ELECTRIC NETWORKS INCLUDING DISTRIBUTED-PARAMETER TRANSMISSION LINE MODELS

Leonardo T. G. Lima
COPPE/UFRJ and UFF
R. Passo da Pátria 156
24.210-240 Niterói, RJ
llima@caa.uff.br

Nelson Martins
CEPEL
C.P. 68007
21.944-970 Rio de Janeiro, RJ
nelson@fund.cepel.br

Sandoval Carneiro Jr.
COPPE/EE/UFRJ
C.P. 68504
21.945-504 Rio de Janeiro, RJ
sandoval@coep.ufrj.br

Abstract - **This paper presents a methodology to obtain a dynamic model of power system networks through the use of an augmented state-space equation. Both lumped and distributed parameters models can be used to represent electric network components. The dynamic model of a linear network of any topology and dimension can be easily obtained and several linear systems techniques can be efficiently applied due to the sparsity of the matrices. This methodology can be used to obtain reduced order equivalent models or to perform harmonic studies.**

Keywords: Electromagnetic Transients Analysis, Power System Modeling, Dynamic Equivalents, Linear Systems, Dominant Poles, Transfer Functions

1. INTRODUCTION

Linear systems techniques, such as frequency response, eigenvalue/eigenvector analysis, sensitivities, transfer function residues, etc., have been successfully applied to the analysis of linearized electro-mechanical stability problems of power systems [1, 2]. These techniques are based on a state-space model and can be readily applied to the analysis of linear aspects of electromagnetic transient phenomena, such as harmonic resonances or reduced order equivalent systems.

The state variables definition for an electric network is not a trivial task. The choice of the currents through inductors and voltages across capacitors is straightforward, but does not assure a minimum set of linear independent variables, which is the necessary condition to form a state-space description of a dynamic system [3].

A previous paper introduced the use of an augmented set of equations to model single-phase networks composed of lumped parameters (RLC) branches and distributed, frequency dependent parameters, transmission lines [4]. Reduced order equivalents were then derived applying the dominant pole concept [1, 2]. The technique is expanded in this paper to three-phase systems including distributed parameter transmission line models, with or without frequency-dependent parameters.

The time and frequency responses obtained through the use of the proposed methodology are then compared with those obtained with EMTP simulations.

2. PROBLEM FORMULATION

Kirchoff's voltage and current laws are, essentially, linear relationships among variables. These topological restrictions may pose a problem to the definition of the state variables of a practical electric network [3]. One simple way to overcome this problem is to adopt a generalized state-space model, the descriptor system [5], written as

$$\begin{aligned} \mathbf{T}\dot{\mathbf{x}} &= \mathbf{A}\,\mathbf{x} + \mathbf{B}\,\mathbf{u} \\ \mathbf{y} &= \mathbf{C}\,\mathbf{x} + \mathbf{D}\,\mathbf{u} \end{aligned} \tag{1}$$

where the matrix **T** is singular.

Descriptor systems allow the simultaneous use of both differential and algebraic equations and this will be used to explicitly include the Kirchoff's current law, written for each node of the network, in the model. Fig. 1 shows the general structure of the descriptor system proposed by the authors [4] to model electric networks.

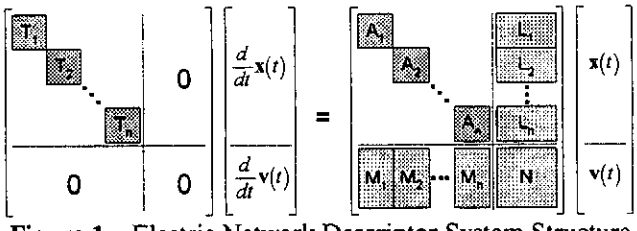

Figure 1 – Electric Network Descriptor System Structure

The vector **x** is the state vector and **v** is the vector of nodal voltages. Each network component will be represented by a set of differential and algebraic equations written as

$$\mathbf{T}_i\dot{\mathbf{x}}_i = \mathbf{A}_i\,\mathbf{x}_i + \mathbf{L}_i\,\mathbf{v} \tag{2}$$

and the currents injected in its terminal nodes are written as

$$\mathbf{I}_i = \mathbf{M}_i\mathbf{x}_i + \mathbf{N}_i\mathbf{v} \tag{3}$$

The current injections in all nodes are equal zero, which is represented in the second set of equations shown in Fig. 1.

2.1. Single-Phase RLC Branch

The basic lumped parameter element used to model electric networks is the RLC branch shown in Fig. 2. This branch is modeled by the following equations:

$$V_k - V_j = R\,I_{kj} + L\frac{dI_{kj}}{dt} + V_c \tag{4}$$

$$C\frac{dV_C}{dt} = I_{kj} \tag{5}$$

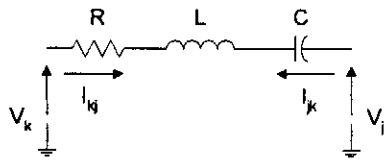

Figure 2 – Lumped RLC single-phase branch

Equations (4) and (5) can be written together in the form shown in equation (2) as

$$\begin{bmatrix} L & 0 \\ 0 & C \end{bmatrix}\begin{bmatrix} \dot{I}_{kj} \\ \dot{V}_C \end{bmatrix} = \begin{bmatrix} -R & -1 \\ 1 & 0 \end{bmatrix}\begin{bmatrix} I_{kj} \\ V_C \end{bmatrix} + \begin{bmatrix} 1 & -1 \\ 0 & 0 \end{bmatrix}\begin{bmatrix} V_k \\ V_j \end{bmatrix} \tag{7}$$

and the current injections on nodes k and j are given by

$$\begin{bmatrix} I_{kj} \\ I_{jk} \end{bmatrix} = \begin{bmatrix} 1 & 0 \\ -1 & 0 \end{bmatrix}\begin{bmatrix} I_{kj} \\ V_C \end{bmatrix} + \begin{bmatrix} 0 & 0 \\ 0 & 0 \end{bmatrix}\begin{bmatrix} V_k \\ V_j \end{bmatrix} \tag{8}$$

These equations also apply when the resistance or the inductance are neglected. On the other hand, when there is no capacitance in the branch, equation (5) should be replaced by $V_C = 0$ and equation (7) modified accordingly:

$$\begin{bmatrix} L & 0 \\ 0 & 0 \end{bmatrix}\begin{bmatrix} \dot{I}_{kj} \\ \dot{V}_C \end{bmatrix} = \begin{bmatrix} -R & -1 \\ 0 & 1 \end{bmatrix}\begin{bmatrix} I_{kj} \\ V_C \end{bmatrix} + \begin{bmatrix} 1 & -1 \\ 0 & 0 \end{bmatrix}\begin{bmatrix} V_k \\ V_j \end{bmatrix} \tag{9}$$

2.2. Transformer

The transformer is represented, in this paper, by a linear model based on single-phase units. Fig. 3 shows the equivalent circuit of the single-phase model.

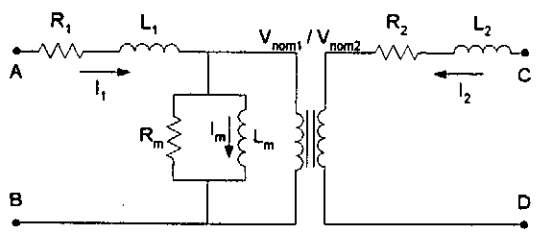

Figure 3 – Equivalent Circuit of the Transformer Model

The following differential equations apply to this model:

$$\begin{aligned} L_1\frac{dI_1}{dt} + R_1 I_1 &= V_A - V_B - V_1 \\ L_2\frac{dI_2}{dt} + R_2 I_2 &= V_C - V_D - V_2 \\ L_m\frac{dI_m}{dt} &= V_1 \end{aligned} \tag{10}$$

and the ideal transformer relations on voltages and currents can be expressed as algebraic equations:

$$V_1 - \frac{V_{nom1}}{V_{nom2}}V_2 = 0 \tag{11}$$

$$I_1 - I_m - \frac{V_1}{R_m} + \frac{V_{nom2}}{V_{nom1}}I_2 = 0 \tag{12}$$

These equations can be written in the matrix form shown in equation (2) where

$$\mathbf{T}_i = \begin{bmatrix} L_1 & 0 & 0 & 0 & 0 \\ 0 & L_2 & 0 & 0 & 0 \\ 0 & 0 & L_m & 0 & 0 \\ 0 & 0 & 0 & 0 & 0 \\ 0 & 0 & 0 & 0 & 0 \end{bmatrix} \tag{13}$$

$$\mathbf{A}_i = \begin{bmatrix} -R_1 & 0 & 0 & -1 & 0 \\ 0 & -R_2 & 0 & 0 & -1 \\ 0 & 0 & 0 & 1 & 0 \\ 0 & 0 & 0 & -1 & V_{nom1}/V_{nom2} \\ 1 & V_{nom1}/V_{nom2} & -1 & -1/R_m & 0 \end{bmatrix} \tag{14}$$

$$\mathbf{L}_i = \begin{bmatrix} 1 & -1 & 0 & 0 \\ 0 & 0 & 1 & -1 \\ 0 & 0 & 0 & 0 \\ 0 & 0 & 0 & 0 \\ 0 & 0 & 0 & 0 \end{bmatrix} \tag{15}$$

with the state vector defined as $\mathbf{x}_i = [I_1\ I_2\ I_m\ V_1\ V_2]^t$ and the terminal voltages $\mathbf{v} = [V_A\ V_B\ V_C\ V_D]^t$.

The injected currents are given by

$$\begin{bmatrix} I_A \\ I_B \\ I_C \\ I_D \end{bmatrix} = \begin{bmatrix} +1 & 0 & 0 & 0 & 0 \\ -1 & 0 & 0 & 0 & 0 \\ 0 & +1 & 0 & 0 & 0 \\ 0 & -1 & 0 & 0 & 0 \end{bmatrix}\begin{bmatrix} I_1 \\ I_2 \\ I_m \\ V_1 \\ V_2 \end{bmatrix} + \begin{bmatrix} 0 & 0 & 0 & 0 \\ 0 & 0 & 0 & 0 \\ 0 & 0 & 0 & 0 \\ 0 & 0 & 0 & 0 \end{bmatrix}\begin{bmatrix} V_A \\ V_B \\ V_C \\ V_D \end{bmatrix} \tag{16}$$

2.3. Three-Phase RLC Branch

The three-phase RLC model allows the representation of coupling effects that exist in three-phase systems. Fig. 4 shows a schematic diagram of this model.

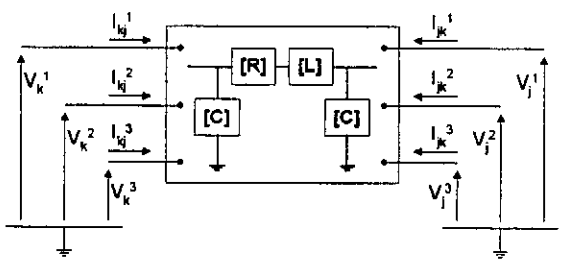

Figure 4 – Three-Phase RLC Lumped Parameter Branch

The following matrix equations are used in this model:

$$\mathbf{v}_k^C - \mathbf{v}_j^C = \mathbf{R}\,\mathbf{i} + \mathbf{L}\frac{d}{dt}\mathbf{i} \tag{17}$$

$$\mathbf{i}_k = \mathbf{C}\frac{d}{dt}\mathbf{v}_k^C + \mathbf{i} \tag{18}$$

$$\mathbf{i}_j = \mathbf{C}\frac{d}{dt}\mathbf{v}_j^C - \mathbf{i} \tag{19}$$

where $\mathbf{i}=[I_1\ I_2\ I_3]^t$ is the vector of the currents through the inductive branches, $\mathbf{v}_k^C$ and $\mathbf{v}_j^C$ are the vectors of nodal voltages across the capacitive branches at terminals k and j, respectively. The vectors $\mathbf{i}_k$ and $\mathbf{i}_j$ are the injected currents at terminals k and j, respectively.

These equations can also be written in the needed matrix form previously outlined in equation (2):

$$\begin{bmatrix} \mathbf{L} & \mathbf{0} & \mathbf{0} & \mathbf{0} & \mathbf{0} \\ \mathbf{0} & \mathbf{C} & \mathbf{0} & \mathbf{0} & \mathbf{0} \\ \mathbf{0} & \mathbf{0} & \mathbf{C} & \mathbf{0} & \mathbf{0} \\ \mathbf{0} & \mathbf{0} & \mathbf{0} & \mathbf{0} & \mathbf{0} \\ \mathbf{0} & \mathbf{0} & \mathbf{0} & \mathbf{0} & \mathbf{0} \end{bmatrix} \frac{d}{dt} \begin{bmatrix} \mathbf{i} \\ \mathbf{v}_k^C \\ \mathbf{v}_j^C \\ \mathbf{i}_k \\ \mathbf{i}_j \end{bmatrix} = \begin{bmatrix} -\mathbf{R} & \mathbf{I} & -\mathbf{I} & \mathbf{0} & \mathbf{0} \\ -\mathbf{I} & \mathbf{0} & \mathbf{0} & \mathbf{I} & \mathbf{0} \\ \mathbf{I} & \mathbf{0} & \mathbf{0} & \mathbf{0} & \mathbf{I} \\ \mathbf{0} & \mathbf{I} & \mathbf{0} & \mathbf{0} & \mathbf{0} \\ \mathbf{0} & \mathbf{0} & \mathbf{I} & \mathbf{0} & \mathbf{0} \end{bmatrix} \begin{bmatrix} \mathbf{i} \\ \mathbf{v}_k^C \\ \mathbf{v}_j^C \\ \mathbf{i}_k \\ \mathbf{i}_j \end{bmatrix} + \begin{bmatrix} \mathbf{0} & \mathbf{0} \\ \mathbf{0} & \mathbf{0} \\ \mathbf{0} & \mathbf{0} \\ -\mathbf{I} & \mathbf{0} \\ \mathbf{0} & -\mathbf{I} \end{bmatrix} \begin{bmatrix} \mathbf{v}_k \\ \mathbf{v}_j \end{bmatrix} \tag{20}$$

Note that the vectors $\mathbf{v}_k^C$ and $\mathbf{v}_j^C$ are equal to the nodal voltages vectors $\mathbf{v}_k$ and $\mathbf{v}_j$, and these algebraic relations are clearly expressed in the 4th and 5th rows of equation (20).

The current injections at the terminal nodes are written as

$$\begin{bmatrix} \mathbf{i}_k \\ \mathbf{i}_j \end{bmatrix} = \begin{bmatrix} \mathbf{0} & \mathbf{0} & \mathbf{0} & \mathbf{I} & \mathbf{0} \\ \mathbf{0} & \mathbf{0} & \mathbf{0} & \mathbf{0} & \mathbf{I} \end{bmatrix} \begin{bmatrix} \mathbf{i} \\ \mathbf{v}_k^C \\ \mathbf{v}_j^C \\ \mathbf{i}_k \\ \mathbf{i}_j \end{bmatrix} + \begin{bmatrix} \mathbf{0} & \mathbf{0} \\ \mathbf{0} & \mathbf{0} \end{bmatrix} \begin{bmatrix} \mathbf{v}_k \\ \mathbf{v}_j \end{bmatrix} \tag{21}$$

2.4. Transmission Line

The distributed parameter transmission line model is based on the modal decomposition of the equations and each propagation mode can be modeled by the equivalent circuit shown in Fig. 5 [6, 7].

The following equations are applied to this equivalent circuit:

$$\begin{aligned} V_k(s) &= B_k(s) + Z_C(s) I_k(s) \\ V_m(s) &= B_m(s) + Z_C(s) I_m(s) \end{aligned} \tag{22}$$

$$\begin{aligned} B_k(s) &= A_1(s)\left[V_m(s) + Z_C(s) I_m(s)\right] \\ B_m(s) &= A_1(s)\left[V_k(s) + Z_C(s) I_k(s)\right] \end{aligned} \tag{23}$$

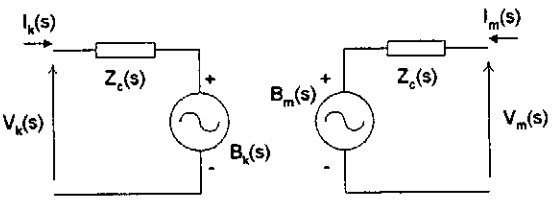

Figure 5 –Transmission Line Modal Equivalent Circuit

This equivalent circuit can be represented by the control system block diagram [8], as shown in Fig. 6.

The frequency-dependent transmission line model proposed in [7] and implemented in the ATP program as the JMARTI setup [9] uses a constant modal transformation matrix and the characteristic impedance $Z_C(s)$ is represented by a rational function approximation given by

$$Z_C(s) \cong R_0 + \sum_{i=1}^{n} \frac{R_{Zi}}{s - \lambda_{Zi}} \tag{24}$$

where λ_{Zi} is a real pole and R_{Zi} is the transfer function residue associated with λ_{Zi}. The term R_0 is a non-zero real constant and is characteristic of a proper transfer function, i. e., a transfer function with the same number of poles and zeros.

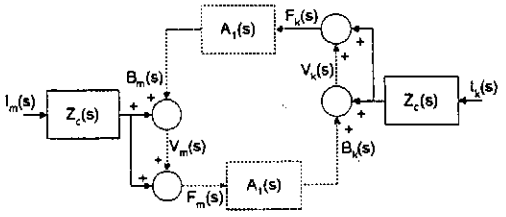

Figure 6 – Transmission Line Modal Block Diagram

The weighting function $A_1(s)$ is represented by a rational transfer function approximation multiplied by the Laplace transform of the ideal time delay τ:

$$A_1(s) \cong e^{-s\tau} P(s) = e^{-s\tau} \sum_{j=1}^{m} \frac{R_{Aj}}{s - \lambda_{Aj}} \tag{25}$$

To obtain a state-space realization of the block diagram shown in Fig. 6, it is necessary to use a rational function approximation of the time delay. This is done by the Padé approximation [8] given by

$$e^{-s\tau} = \frac{2 - \tau s + \dfrac{(-\tau s)^2}{2!} + \dfrac{(-\tau s)^3}{3!} \cdots}{2 + \tau s + \dfrac{(\tau s)^2}{2!} + \dfrac{(\tau s)^3}{3!} \cdots} \tag{26}$$

The modal values shown in Fig. 5 and 6 should be transformed to phase values in order to connect the three-phase transmission line model to the rest of the system. These variable transformations are given by

$$\mathbf{v}^{abc} = \mathbf{T}_v\, \mathbf{v}^{123} \tag{27}$$

$$\mathbf{i}^{abc} = \mathbf{T}_i\, \mathbf{i}^{123} \tag{28}$$

where $\mathbf{v}^{123}$ and $\mathbf{v}^{abc}$ are the vectors of modal and phase voltages. The same notation applies to the current vectors $\mathbf{i}^{123}$ and $\mathbf{i}^{abc}$. It is well known that $[\mathbf{T}_v]^{-1} = [\mathbf{T}_i]^t$.

A three-phase transmission line is modeled by the following equations:

$$\begin{aligned} \dot{\mathbf{x}}'_{z1} &= \mathbf{A}'_{z1}\, \mathbf{x}'_{z1} + \mathbf{b}'_{z1}\, I^i_{km} \\ y'_{z1} &= \mathbf{C}'_{z1}\, \mathbf{x}'_{z1} + d'_{z1}\, I^i_{km} \\ \dot{\mathbf{x}}'_{z2} &= \mathbf{A}'_{z2}\, \mathbf{x}'_{z2} + \mathbf{b}'_{z2}\, I^i_{mk} \\ y'_{z2} &= \mathbf{C}'_{z2}\, \mathbf{x}'_{z2} + d'_{z2}\, I^i_{mk} \end{aligned} \qquad i = 1,\ 2,\ 3 \tag{29}$$

which are the state-space realizations of the transfer function approximation of the characteristic impedance, given in equation (24), for each one of the propagation modes of the transmission line. There are two sets of equations for each mode due to the duplicity of the blocks in the diagram shown in Fig. 6.

The function $P(s)$ defined in equation (25) is represented by

$$\begin{aligned} \dot{\mathbf{x}}^i_{P1} &= \mathbf{A}^i_{P1}\,\mathbf{x}^i_{P1} + \mathbf{b}^i_{P1}\,u^i_{P1} \\ y^i_{P1} &= \mathbf{C}^i_{P1}\,\mathbf{x}^i_{P1} \\ \dot{\mathbf{x}}^i_{P2} &= \mathbf{A}^i_{P2}\,\mathbf{x}^i_{P2} + \mathbf{b}^i_{P2}\,u^i_{P2} \\ y^i_{P2} &= \mathbf{C}^i_{P2}\,\mathbf{x}^i_{P2} \end{aligned} \qquad i = 1,\ 2,\ 3 \qquad (30)$$

where u denotes the input variable of the block and y is its output. Again, there are two sets of equations for each propagation mode.

The time delay is represented by the state-space realization of the Padé approximation given by (26) and the following equations are used in the model:

$$\begin{aligned} \dot{\mathbf{x}}^i_{D1} &= \mathbf{A}^i_{D1}\,\mathbf{x}^i_{D1} + \mathbf{b}^i_{D1}\,u^i_{D1} \\ y^i_{D1} &= \mathbf{C}\,\mathbf{x}^i_{D1} + d^i_{D1}\,u^i_{D1} \\ \dot{\mathbf{x}}^i_{D2} &= \mathbf{A}^i_{D2}\,\mathbf{x}^i_{D2} + \mathbf{b}^i_{D2}\,u^i_{D2} \\ y^i_{D2} &= \mathbf{C}\,\mathbf{x}^i_{D2} + d^i_{D2}\,u^i_{D2} \end{aligned} \qquad i = 1,\ 2,\ 3 \qquad (31)$$

The interconnection between the different state-space blocks is made by algebraic equations. The following relationships can be established from the block diagram of Fig. 6:

$$\begin{aligned} u^i_{P1} &= y^i_{D1} \\ u^i_{P2} &= y^i_{D2} \\ u^i_{D1} &= y^i_{P2} + 2y^i_{Z1} \\ u^i_{D2} &= y^i_{P1} + 2y^i_{Z2} \end{aligned} \qquad i = 1,\ 2,\ 3 \qquad (32)$$

Additionally, the modal voltages can be written as

$$\begin{aligned} V^i_k &= y^i_{P2} + y^i_{Z1} = \begin{bmatrix} t_{1i} & t_{2i} & t_{3i} \end{bmatrix} \mathbf{v}^k_{abc} \\ V^i_m &= y^i_{P1} + y^i_{Z2} = \begin{bmatrix} t_{1i} & t_{2i} & t_{3i} \end{bmatrix} \mathbf{v}^m_{abc} \end{aligned} \qquad i = 1,\ 2,\ 3 \qquad (33)$$

where t_{ij} is the (i,j)-element of the matrix $\mathbf{T}_i$ and $\mathbf{v}_{abc}{}^k$ and $\mathbf{v}_{abc}{}^k$ are the nodal voltages vectors at terminals k and m, respectively.

The current injections at the terminal nodes k and m, referred to phase variables, can be written as

$$\mathbf{i}^k_{abc} = \mathbf{T}_i\,\mathbf{i}^{km}_{123} \qquad (34)$$

$$\mathbf{i}^m_{abc} = \mathbf{T}_i\,\mathbf{i}^{mk}_{123} \qquad (35)$$

where $\mathbf{i}^{km}_{123}$ and $\mathbf{i}^{mk}_{123}$ are the vectors of modal current injections at terminals k and m, respectively.

When the frequency dependency of the transmission line model is neglected, the characteristic impedance Z_C becomes a constant and the function $P(s)$ in (25) is made equal to one. Thus the weighting function $A_1(s)$ will be equal to the Laplace transform of the ideal time delay τ. The functions in the block diagram of Fig. 6 are very much simplified, as shown in Fig. 7.

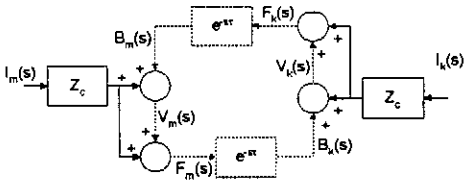

Figure 7 – Modal Block Diagram for Ideal Line

If the losses are neglected, Z_C becomes a real constant and this block diagram will represent a lossless constant parameter single-phase transmission line or a propagation mode of a multi-phase line.

The losses can be taken into account considering two distributed parameter transmission line segments connected by lumped resistances [9].

3. RESULTS

Fig. 8 shows the test system used in this paper. This system was proposed in [10] and was also used in a work developed at COPPE/UFRJ [11].

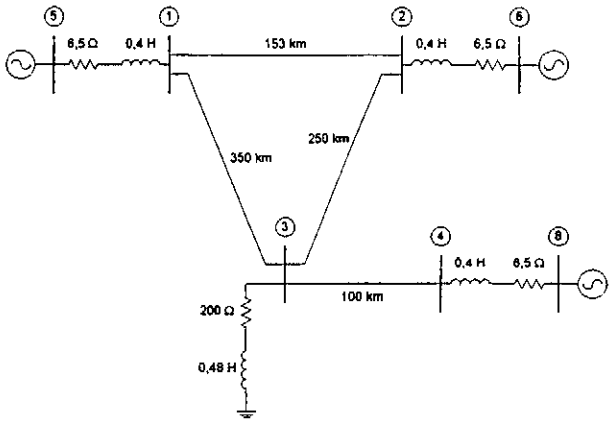

Figure 8 – Test System One-Line Diagram

The objective here is to study the fast transients in the transmission line between buses 3 and 4, when subjected to single-phase short circuits. The system can be partitioned at bus 3, resulting in an study system containing only one transmission line and generation at bus 8 and an external system with 3 transmission lines and 2 generation buses.

All the transmission lines are modeled by frequency-dependent distributed parameter models, using the JMARTI Setup of the ATP program [9] with its default settings. Table 1 shows the order of the rational function approximations produced by ATP.

The external system is to be replaced by a reduced order Norton equivalent located at bus 3.

Fig. 9 shows the frequency response of the transfer functions from the current injected in phase a to the abc voltages at bus 3: $V_{a3}(s)/I_{a3}(s)$, $V_{b3}(s)/I_{a3}(s)$ and $V_{c3}(s)/I_{a3}(s)$. Note that these transfer functions are dimensionally equivalent to impedances.

Table 1 – JMARTI Setup Transmission Line Model

RATIONAL APPROXIMATION ORDER	TRANSMISSION LINE		
	1-2	2-3	1-3
$Z_C(s)$	23	25	24
$P(s)$	16	15	19

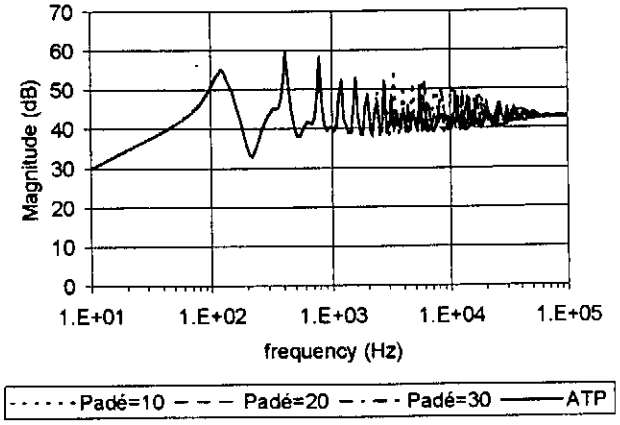

(a). Transfer Function $V_{a3}(s)/I_{a3}(s)$

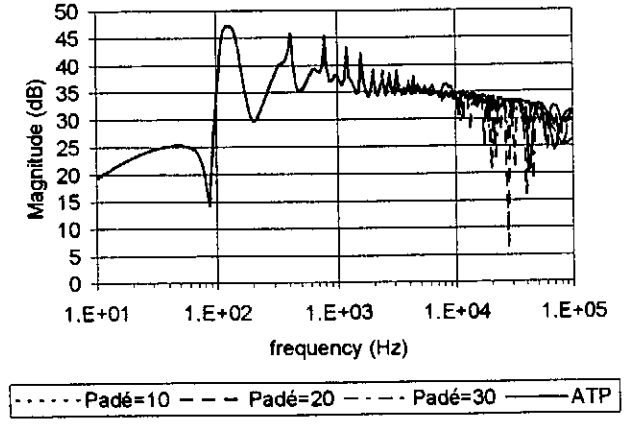

(b). Transfer Function $V_{b3}(s)/I_{a3}(s)$

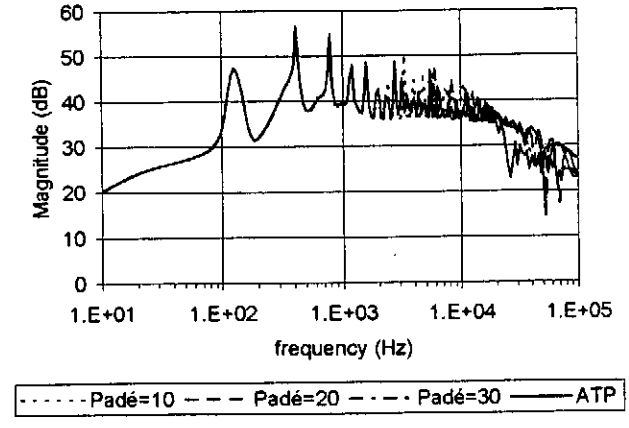

(c). Transfer Function $V_{c3}(s)/I_{a3}(s)$

Figure 9 – Bode Plots of the External System

The solid lines represent the results obtained using frequency scan with the ATP program. They are compared with those obtained with the proposed methodology, considering Padé approximations to the time delay of different orders. The external system was modeled by descriptor systems of dimensions 1050, 1230 and 1410, for Padé approximations of order 10, 20 and 30, respectively.

The Padé approximations were able to correctly represent the frequency response up to a few kHz. If this bandwidth is inadequate to the study objectives, one should use a higher order approximation or adopt an exact frequency representation of the time delay function.

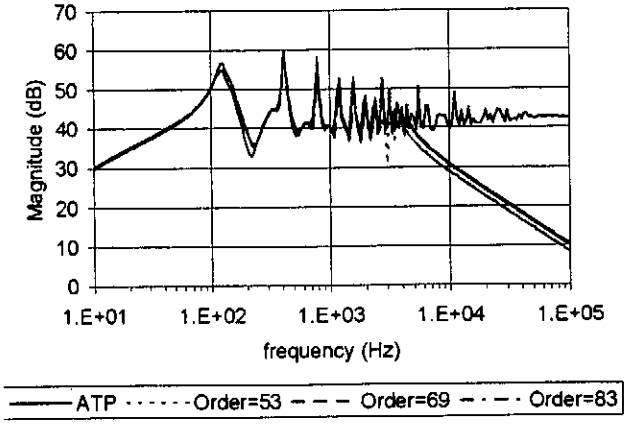

(a). Transfer Function $V_{a3}(s)/I_{a3}(s)$

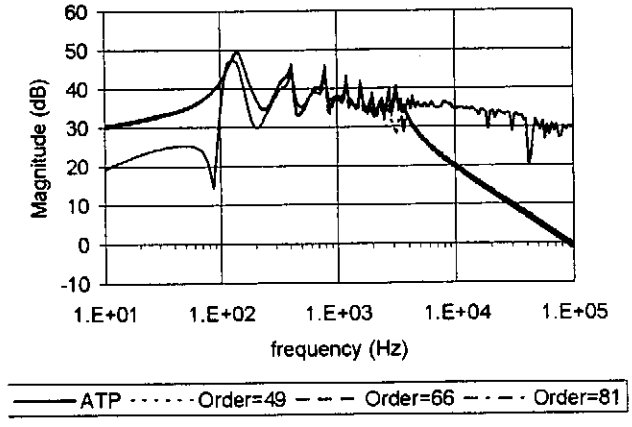

(b). Transfer Function $V_{b3}(s)/I_{a3}(s)$

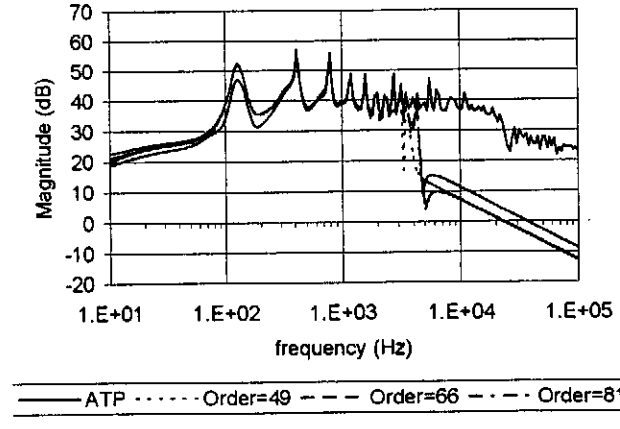

(c). Transfer Function $V_{c3}(s)/I_{a3}(s)$

Figure 10 – Bode Plots of the Reduced Order Model

The dominant poles of the transfer functions shown in Fig. 9 were obtained using the Dominant Pole

Spectrum Eigensolver (DPSE) algorithm, proposed in [2]. Almost 200 poles were obtained, using several runs of the algorithm, with different initial guesses. Sets of 30, 40 and 50 of these poles were selected to form the equivalent reduced order model. Fig. 10 shows the frequency responses of these equivalents, compared with the complete system response, obtained with the ATP program.

It can be seen that the matching of the self-impedance $V_{a3}(s)/I_{a3}(s)$ is better than those obtained for the mutual elements $V_{b3}(s)/I_{a3}(s)$ and $V_{b3}(s)/I_{a3}(s)$, specially in the low frequency range. This is mainly due to a zero on the origin, characteristic of these mutual transfer functions, that was not represented in the reduced order model.

This transfer function zero is important to the time response of the system, since it is responsible for the null steady-state value of the voltages on phases *b* and *c* for a constant current injected on phase *a*. Thus, it should be included on the reduced order model to achieve better time responses. Work is now being carried out to take this effect into account.

4. CONCLUSIONS

An augmented state-space formulation is proposed to the analysis of power system networks transients. This method can cope with linear networks of any order and topology, and distributed-parameter transmission line models can be used together with lumped-parameter branches.

This formulation yields very sparse matrices and efficient algorithms can be applied to obtain frequency responses and time or modal analysis.

The transfer function dominant pole spectrum concept was applied to obtain a reduced order dynamic equivalent that matches the complete system frequency response in a specified frequency range.

A clear advantage of the proposed dynamic equivalents is their ability to properly consider the effects of distributed-parameter frequency-dependent transmission lines.

This formulation can be also applied to harmonic studies, as described in [12].

ACKNOWLEDGMENTS

The first author would like to thank CAPES Foundation, FINEP/RECOPE Project SAGE #0626-96 and the Universidade Federal Fluminense (UFF) for the financial support and leave of absence.

5. REFERENCES

[1] **N. Martins, L. T. G. Lima & H. J. C. P. Pinto** – "Computing Dominant Poles of Power System Transfer Functions", *IEEE Trans. on Power Systems*, vol. PWRS-11, no. 1, pp. 162-170, February, 1996.

[2] **N. Martins** – "The Dominant Pole Spectrum Eigensolver", *IEEE Trans. on Power Systems*, vol. PWRS-12, no. 1, pp. 245-254, February 1997.

[3] **Leon O. Chua & Pen M. Lin** - *Computer-Aided Analysis of Electronic Circuits: Algorithms and Computational Techniques*, Prentice-Hall, Inc., NJ, USA, 1975.

[4] **Leonardo T. G. Lima, Nelson Martins & Sandoval Carneiro Jr.** – "Dynamic Equivalents for Electromagnetic Transient Analysis Including Frequency-Dependent Transmission Line Parameters", *Proceedings of International Conference on Power Systems Transients IPST'97*, pp. 131-136, Seattle, USA, 1997.

[5] **David G. Luenberger** - "Dynamic Equations in Descriptor Form", *IEEE Trans. On Automatic Control*, vol. AC-22, no. 3, pp. 312-321, June 1977.

[6] **Hermann W. Dommel** - "Digital Computer Solution of Electromagnetic Transients in Single- and Multi-Phase Networks", *IEEE Trans. On Power Apparatus and Systems*, vol. PAS-88, April, 1969, pp.388-399, reprinted in *Computer Analysis of Electric Power System Transients – Selected Readings*, pp. 11-22, ed. **Juan A. Martinez-Velasco**, IEEE Press, USA, 1997.

[7] **José R. Marti** – "Accurate Modelling of Frequency-Dependent Transmission Lines in Electromagnetic Transient Simulations", *IEEE Trans. on Power Apparatus and Systems*, vol. PAS-101, no. 1, January 1982, pp. 147-155.

[8] **Benjamin C. Kuo** - *Automatic Control Systems*, 6th ed., Prentice-Hall International, Inc., Englewood Cliffs, NJ, USA, 1991.

[9] **Leuven EMTP Center** - *Alternative Transients Program Rule Book*, Heverlee, Belgium, Julho, 1987.

[10] **A. S. Morched & V. Brandwajn** – "Transmission Network Equivalents for Electromagnetic Transients Studies", *IEEE Trans. on Power Apparatus and Systems*, vol. PAS-102, no. 9, pp. 2984-2994, September, 1983.

[11] **Clever Sebastião Pereira Filho** – *Digital Filter Equivalents for Real-Time Transient Simulation of Electric Power Systems*, Ph.D. Thesis, COPPE/UFRJ, Brasil, December, 1997 (in portuguese).

[12] **Sérgio L. Varricchio, Nelson Martins, Leonardo T. G. Lima & Sandoval Carneiro Jr.** – "Studying Harmonic Problems Using a Descriptor System Approach", *submitted to International Conference on Power Systems Transients IPST'99*, Hungary, June, 1999.